Tissue Average Binding and Equilibrium Distribution: An Example with Heparin in Arterial Tissues

Mark A. Lovich* and Elazer R. Edelman*‡

*Harvard University-Massachusetts Institute of Technology, Division of Health Sciences and Technology, Cambridge, Massachusetts 02139, and ‡Department of Internal Medicine, Cardiovascular Division, Brigham and Women's Hospital, Harvard Medical School, Boston, Massachusetts USA

ABSTRACT Classical pharmacokinetic descriptions do not adequately predict the dynamic and complex drug deposition patterns that follow some novel delivery techniques, in part because they do not characterize binding within intact tissues in sufficient detail. In this study, the binding site density of all the potential sites, the tissue-average dissociation constant, and the fractional volume in which heparin can distribute in arterial tissues were measured by incubating tissue samples to equilibrium in solutions containing a wide range of drug concentrations. An "equilibrium distribution curve" was constructed by plotting the concentration of drug in each sample against the concentration in the corresponding bulk phase. The above constants were determined by computationally fitting this curve to a model of drug distribution within tissues. The binding site density was measured to be 4.2 μM, 2.5 μM, and 2.2 nM in porcine carotid media with intact and denuded endothelium, and adventitia, respectively. The dissociation constant of heparin in these tissues was estimated to be 6.8 μM, 5.0 μM, and 8.1 nM, respectively. The fractional tissue volume of distribution was 0.61, 0.70, and 0.87, respectively. These values are consistent with known properties of the heparin-arterial tissue interaction. Thus, this technique describes the cumulative effects of binding of a compound to all of its potential binding sites, and will be essential to new detailed descriptions of drug distribution.

INTRODUCTION

The hyperproliferative vascular response to injury is the greatest limitation to the potential of mechanical revascularization (Ip et al., 1990). Up to 50% of angioplasty patients must undergo a second procedure within 3–6 months (Ellis et al., 1988), and now that immune rejection has been partially treated with suppressants, more than half of the heart transplants fail because of accelerated arteriosclerosis (Ip et al., 1990). Much has been learned about the biology of these diseases from tissue culture experiments, including the principal cell types involved in this process and the role of growth factors and receptors, glycoproteins, metalloproteases, selectins, etc. These studies have suggested classes of compounds and specific agents that might be used to combat these diseases, and yet none of these agents work in the clinic. One of the limitations of extrapolating from tissue culture data to clinical trials is the inadequacy of pharmacokinetic understanding and detailed modeling of the distribution for compounds. The binding of a single ligand to a specific receptor describes events well in culture but is clearly only a small part of all the physical interactions in an intact tissue. These interactions include binding of drug to nonspecific binding sites, idiosyncratic binding to different tissue elements, differential functions of soluble and bound drug, and gradients in concentration imposed by various means of administration to tissues. Heparin is a perfect example of these phenomena. This polysaccharide is the gold standard inhibitor of cultured vascular smooth muscle cells (Castellot et al., 1981, 1985a, 1987), but if anything it is an exacerbating agent in human disease (Ellis et al., 1989; Lehmann et al., 1991). Recent data from our laboratory demonstrated that its in vivo effects are remarkably sensitive to the mode of administration (Edelman et al., 1990; Rogers et al., 1993; Edelman and Karnovsky, 1994). Furthermore, intermittent heparin dosing can exacerbate disease, whereas continuous administration will alleviate it (Edelman and Karnovsky, 1994). Thus, a more mathematically rigorous pharmacokinetic model of drug distribution is needed to correlate the mode of delivery with the biological efficacy of drugs such as heparin.

Previously we examined the forces of heparin transport within the blood vessel wall and measured the diffusivity of heparin in different arterial layers (Lovich and Edelman, 1995). Detailed descriptions of drug deposition, however, rely to an equal extent on drug binding to intact tissues. In this study we present a novel and quantitative approach to characterizing the binding of heparin to arterial tissues, in terms of binding site density, tissue-average dissociation constant, and fractional volume of tissue in which drug can distribute. This technique attempts to fill the voids listed above by quantifying both biologically active and nonspecific binding, discriminating bound from soluble fractions of drug in tissues, and allowing for drug concentration gradients across tissues when combined with transport data in future computational pharmacokinetic models. Although validated here with heparin, the method is applicable to many drugs and tissues.

Received for publication 25 october 1995 and in final form 20 December 1995.

Address reprint requests to Dr. Mark A. Lovich, Division of Health Sciences and Technology, Massachusetts Institute of Technology, 20A-129, Cambridge, MA 02139. Tel.: 617-252-1655; Fax: 617-253-2514; E-mail: lovich@mit.edu.

0006-3495/96/03/1553/07 $2.00

EQUILIBRIUM DISTRIBUTION MODEL

The equilibrium distribution technique measures the binding and distribution constants by incubating many samples of tissues in solutions with a wide range of radiolabeled drug concentrations and curve-fitting the resulting data to the following model. The model is derived in general terms and should be applicable to many compounds and tissues. The total concentration of drug observed within a volume of tissue (c_T) is considered to be the superposition of soluble (c_s) and bound drug to both cell surface and extracellular matrix binding sites (c_b):

$$c_T = c_s + c_b. \tag{1}$$

At very low drug concentrations, an increase in total concentration results in a linear increase in both soluble and bound concentrations (Fig. 1). As binding sites saturate, increases in the total concentration will be solely noted as increases in the soluble concentration. In a unit volume of tissue there are regions where soluble drug is excluded by steric interactions. The fractional volume in which drug can distribute (ϵ) is given by:

$$\epsilon = \frac{V_a}{V_T}, \tag{2}$$

where V_a is the accessible space for drug distribution and V_T is the total tissue volume. Note that the convention used in this work is that the drug concentrations c_T, c_s, and c_b are defined as the moles of drug per unit total volume of tissue. Thus, the moles of soluble drug per unit total volume of tissue (c_s) is related to the moles of soluble drug per unit accessible volume (c_a) by the fractional volume:

$$c_s = \epsilon c_a. \tag{3}$$

The law of mass action defines the dissociation constant (K_d) as the product of the drug concentration in the accessible volume and the ratio of the molar densities of free (B_f) and bound (B_b) binding sites:

$$K_d = \frac{c_a B_f}{B_b}. \tag{4}$$

The number of binding sites is assumed to be conserved so that the total binding site density (B_T) can be expressed as

$$B_T = B_f + B_b. \tag{5}$$

Although in the context of the law of mass action these binding site densities should be defined as moles of binding sites per unit accessible volume, because the bound and free densities are related as in Eq. 4, they can be and are defined per unit total volume. By assuming a 1:1 bound ligand-to-occupied binding site ratio:

$$c_b = B_b. \tag{6}$$

By combining Eqs. 1, 3–6:

$$c_T = \epsilon c_a + \frac{B_T c_a}{K_d + c_a}. \tag{7}$$

Equilibrium distribution measurements

In these equilibrium distribution measurements, the concentration of drug in the accessible volume (c_a) is established by incubating the tissues in solutions containing radiolabeled drug until equilibrium. The concentration of drug in the accessible volume (c_a), however, is not necessarily equal to the external or bulk phase concentration (c_{bulk}) because of potential charged partitioning. Thus:

$$c_{bulk} = \kappa c_a, \tag{8}$$

where κ is the partition coefficient of drug into the accessible volume. Thus:

$$c_T = \frac{\epsilon}{\kappa} c_{bulk} + \frac{c_{bulk} B_T}{\kappa K_d + c_{bulk}}. \tag{9}$$

The dissociation constant and the partition coefficient are combined into a modified dissociation constant reflecting binding and charged association:

$$K' = \kappa K_d. \tag{10}$$

Similarly, a modified fractional volume of distribution reflecting sterical and charged effects can be defined:

$$\epsilon' = \frac{\epsilon}{\kappa}. \tag{11}$$

Thus:

$$c_T = \epsilon' c_{bulk} + \frac{c_{bulk} B_T}{K' + c_{bulk}}. \tag{12}$$

Thus, the total concentration is a function of the concentration outside the tissue, and this nonlinear relationship depends on the three binding and distribution constants, which are specific to each drug and tissue.

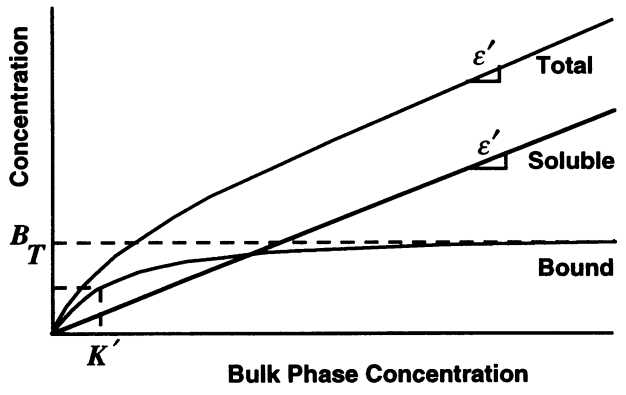

FIGURE 1 Model of drug distribution through tissues at equilibrium. The total concentration is the sum of the bound and soluble fractions. The soluble concentration increases linearly with external or bulk phase concentration, whereas the bound fraction saturates.

Curve fitting and initial estimates

A commercially available nonlinear least-squares Levenberg-Marquardt algorithm including a Pearson minimization (TableCurve 2D, Jandel Scientific, San Rafael, CA) was used to fit the data and determine the binding and distribution constants (ϵ', B_T, and K'). Because the bulk phase concentration data must span many orders of magnitude, a fit to Eq. 12 would preferentially weight the data taken at the highest bulk phase concentrations. The inherent weighting can be distributed over all of the data points by fitting the logarithm of the measured total concentration (c_T) to the following equation:

$$\ln(c_T) = \ln\left(\epsilon' c_{bulk} + \frac{c_{bulk} B_T}{K' + c_{bulk}}\right). \quad (13)$$

Nonlinear least-squares algorithms are sensitive to the initial estimates of the unknown constants (Press et al., 1986). The following approximate method for determining ϵ', B_T, and K' from the equilibrium distribution curve is used to provide the initial estimates for the curve fit. Consider an idealized equilibrium distribution curve that is the sum of the bound and soluble drug (Fig. 1). A least-squares estimate of the slope (ϵ') at high bulk phase concentrations allows the soluble component of the data ($\epsilon' c_{bulk}$) to be subtracted from the total concentration data, reducing Eq. 12 to

$$c_b = \frac{c_{bulk} B_T}{K' + c_{bulk}}. \quad (14)$$

The resulting plateau can be considered equivalent to the total number of binding sites. The average dissociation constant can be estimated as the bulk phase concentration at which half of the binding sites are occupied.

The reliability of the commercial software was assessed by writing an alternative curve-fitting program utilizing a Nelder-Meade function-minimization routine (Matlab, Math Works, Natick, MA). All of the constants computed by the former algorithm differed maximally from the later by 8%, thus validating the former.

Bound and soluble fractions

The equilibrium distribution method also allows for the total concentration measurement (c_T) to be resolved into bound and soluble components. By combining Eqs. 3, 7, 10, and 11:

$$c_s = \frac{c_T - B_T - K'\epsilon' + \sqrt{(c_T - B_T - K'\epsilon')^2 + 4c_T K'\epsilon'}}{2}. \quad (15)$$

The distinction between bound and soluble drug is important. Although soluble drug binds to active receptors and mediates extracellular signaling events, nonspecific binding sites play a distinct role, as they sequester drug in the vicinity of active receptors (Nugent and Edelman, 1992; Edelman et al., 1993). Furthermore, in terms of drug distribution and pharmacokinetics, only the soluble fraction of drug is available to diffuse or convect through a tissue, whereas potential binding sites tend to impede the movement of drug.

EXPERIMENTAL METHODS

The equilibrium distribution method described above was used to determine the binding and distribution constants (B_T, k', and ϵ') for heparin in porcine carotid media with endothelium intact and after endothelial denudation, and in the adventitia. Porcine carotid arteries were explanted and stored on ice for no more than 2 h. The adventitia was stripped from the media, and both were temporarily stored in 2% penicillin-streptomycin (Gibco, Gaithersburg, MD) in sterile phosphate buffered saline. The endothelium of some of these arteries were denuded with three passes of an inflated 3 French embolectomy catheter (Baxter, McGaw Park, IL) (Clowes et al., 1983). Arteries were cut into 10–40-mg pieces and incubated in Dulbecco's modified Eagle's medium (Gibco) with 10% fetal bovine serum (Gibco) and 2% penicillin-streptomycin, with [^{3}H]heparin (Dupont-NEN, Wilmington, DE) concentrations ranging from approximately 100 pM to 0.2 mM. All incubations were performed in 2 ml of culture medium and were carried out until equilibrium, which was achieved when the time rate of increase of drug concentration in the tissue reached zero. After incubation, the arterial specimens were blotted on dry towels, weighed wet, solubilized, and scintillation counted. At least four pieces of each type of tissue were incubated at each bulk phase concentration (c_{bulk}). Bulk phase heparin concentration measurements were made at the end of the incubations and were the average of three 50-μl samples from each culture well. These equilibrium distribution measurements were repeated twice for each tissue type, using different batches of reagents. Histological frozen sections were taken from representative arteries for morphological evaluation.

Prior to the above experiments, the time course of heparin equilibration was quantified in samples of porcine carotid media with endothelium by incubating in a bulk phase concentration of 0.15 mg/ml (Fig. 2). Although vascular cells and interstitial molecules may continue to exchange drug with the bulk phase, these data show that heparin reaches equilibrium with the tissue as a whole well within 24 h. All subsequent incubations were therefore carried out for this duration. In separate experiments, the density of fresh porcine carotid media was measured using a micro-graduated cylinder and an analytical balance. The resulting density of 0.983 ± 0.024

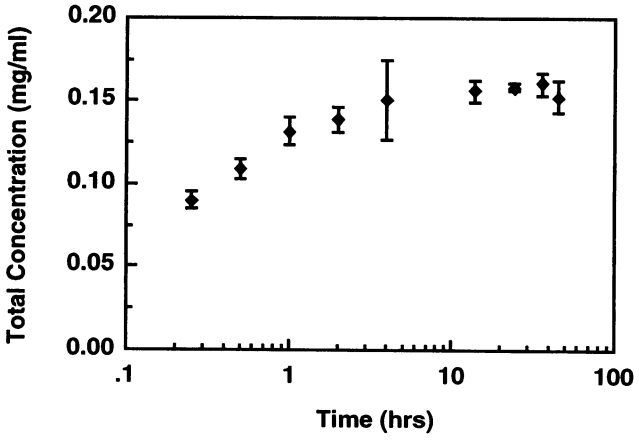

FIGURE 2 Total concentration of porcine carotid media over time when incubated in 0.15 mg/ml heparin. Equilibrium is achieved in less than 24 h (average ± standard error, n = 4).

g/ml (n = 5, ± standard deviation) was used to convert wet weight to volume for calculations of total drug concentration in tissue.

VERIFICATION OF THE EQUILIBRIUM DISTRIBUTION METHOD

Equilibrium distribution data are shown for arterial media with intact and denuded endothelium and adventitia (Fig. 3). Each point shown represents the average (± standard error) of at least four total concentration measurements on samples of tissue from the same culture well and three measurements of the bulk phase concentration in that well. Note that the error bars are present but unappreciable on the logarithmic scale. For each tissue type, initial estimates of the fractional volume of tissue in which drug can distribute (ϵ') were determined through linear regression of the high bulk phase concentration data ($c_{bulk} > 10^{-5}$ M; Table 1). Fig. 4 shows all of these data after the subtraction of the soluble fraction of drug ($\epsilon' c_{bulk}$). For arterial media with intact and denuded endothelium, initial estimates of the binding site density (B_T) were estimated as the plateau of these curves. The dissociation constant of the average binding site (K') was estimated as the bulk phase concentration where half of the binding sites were saturated. The Levenberg-Marquardt curve-fit algorithm converged to the solutions shown (Table 2) when the initial estimates (Table 1) were used and when these initial estimates were perturbed up or down by two orders of magnitude for B_T and K', and by 0.2 for ϵ', for arterial media with intact and denuded endothelium. This curve-fit software also calculated standard errors for each binding and distribution constant. These fits were further assessed by computing best-fit curves for the experimental data and the computed bound concentrations using Eqs. 12 and 14, respectively (Figs. 3 and 4, *solid lines*). It was not possible to obtain initial estimates of B_T and K' for the adventitia because the bound concentration spread about zero after the subtraction of the linear soluble component (Fig. 4 *c*). This indicated that the binding site density in this tissue was lower than the scatter in the data at high bulk phase concentrations. Despite this, the curve-fit algorithm converged on binding constants for the adventitia (Table 2) that were consistent over a wide range of assumed initial estimates.

The equilibrium distribution analysis for heparin within arterial tissues predicts observed heparin-vascular tissue interactions. The fractional volume of tissue in which a drug can distribute (ϵ') is highest in the adventitia and increases in the arterial media after balloon denuding injury (Table 2), reflecting the loose architecture and high content of connective tissues of the former (Murata et al., 1986; Haas et al., 1991) and the role of structural damage in the latter. The analysis also shows that the concentration of binding sites (B_T) in the arterial wall is larger with intact endothelium, consistent with many reports that this monolayer binds heparin (Glimelius et al., 1978; Barzu et al., 1985, 1986; Vannucchi et al., 1986; Psuja, 1987; Hiebert and McDuffie, 1989). In addition, cultured endothelial cells possess nearly

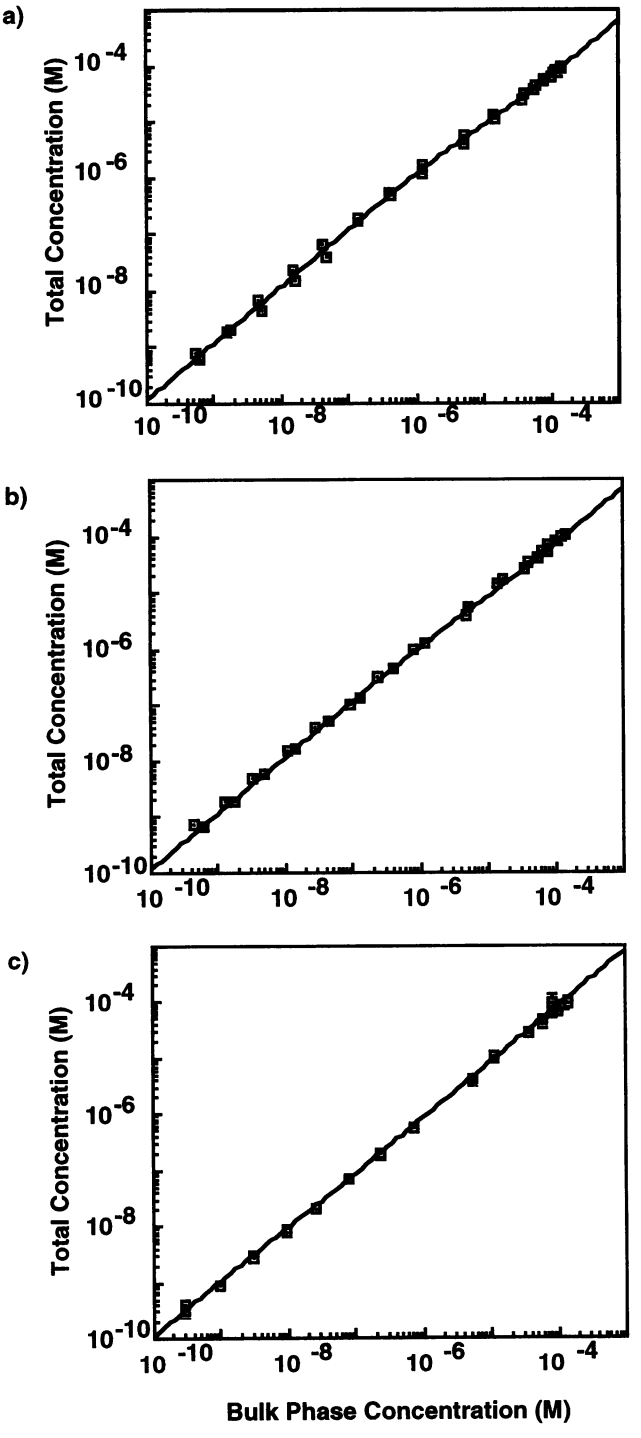

FIGURE 3 Measured equilibrium distribution curves for heparin within (*a*) arterial media with endothelium, (*b*) denuded media, and (*c*) adventitia (average ± standard error, $n > 4$). Solid lines are generated from the curve fit binding and distribution constants (ϵ', B_T, and K') shown in Table 2 and Eq. 12.

100-fold more heparin binding sites than cultured vascular smooth muscle cells (Castellot et al., 1985b; Psuja, 1987). Thus, it is plausible that the presence of the endothelium may nearly double the number of heparin binding sites on a

TABLE 1 Sample binding and distribution constants*

	ϵ'	B_T (μM)	K' (μM)
Arterial media with intact endothelium	0.60	4	12
Arterial media with denuded endothelium	0.63	8	10
Adventitia	0.78	—	—

*Determined by 1) finding the slope (ϵ') of the equilibrium distribution data (Fig. 3) for $c_{bulk} > 10^{-5}$ M; 2) subtracting $\epsilon' c_{bulk}$ from the data and replotting (Fig. 4); 3) approximating B_T as the plateau of the subsequent data; and 4) approximating K' as c_{bulk} at $B_T/2$. Note that B_T and K' were too low to be estimated in the adventitia.

large 250-μm-thick artery as we report. The dissociation constant of the average binding site (K') of the arterial media, assuming a partition coefficient of 1, is three orders of magnitude higher than for growth-arrested smooth muscle cells and basic fibroblast growth factor (Castellot et al., 1985b; San Antonio et al., 1993), and about one to two orders of magnitude higher than laminin, fibronectin, and type I collagen (San Antonio et al., 1993), indicating that much of the binding is to arterial elements with even lower affinity. The dissociation constant (K') of the arterial media is much higher than that of the adventitia, indicating that although there are far fewer binding sites in the latter, they are of much higher affinity. This may be explained by the large concentration of type I collagen in the adventitia (Murata et al., 1986; Haas et al., 1991), whose affinity for heparin is about the same as the values we report here for the adventitia (San Antonio et al., 1993), and the relative scarcity of cells and hence cell surface binding sites. These trends are consistent with known properties of the heparin-arterial tissue interaction and help validate the equilibrium distribution technique.

DISCUSSION

We sought to create a quantitative description of how drugs distribute and bind to intact tissues, with the hope of incorporating these findings into new detailed pharmacokinetic models. This new equilibrium distribution analysis quantifies drug binding to all its potential binding sites, distinguishes between soluble and bound components of drug concentration, and allows for large gradients in deposited drug. This was accomplished by incubating many samples of tissue in solutions containing a wide range of drug concentrations, measuring the corresponding tissue concentrations, and computationally fitting these data to a model of drug distribution and binding. In this way, the binding site density, dissociation constant of the average binding site, and fractional volume of drug distribution were measured for heparin in arterial tissues, and these results were used to validate the technique.

Two methods of determining the binding and distribution constants (ϵ', B_T, and K') from an equilibrium distribution curve have been described. The first requires a linear regression of the data, algebra, and visual inspection. Although this method is relatively simple, it affords no assessment of the "goodness of fit" or statistical measure of accuracy. In addition, errors in estimating ϵ' are carried

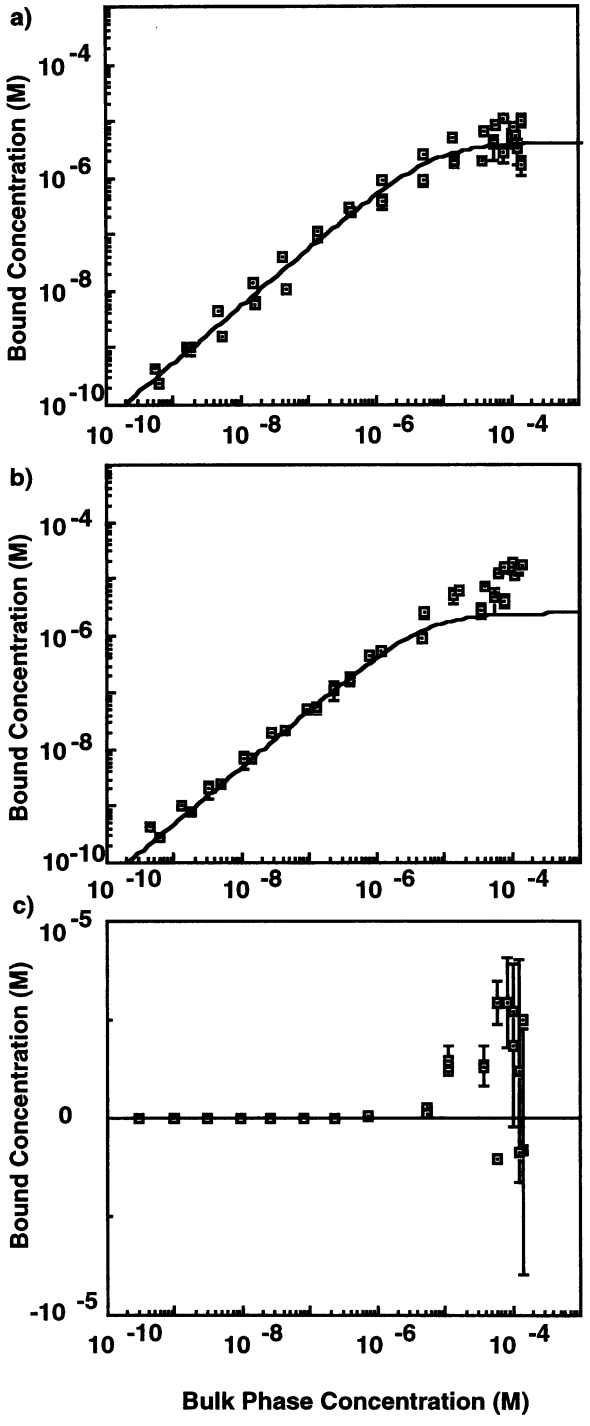

FIGURE 4 Bound concentration of drug in the tissue (c_b) for (*a*) arterial media with endothelium, (*b*) denuded media, and (*c*) adventitia, determined by subtracting the soluble (c_s) fraction from the total concentration (c_T). The plateau corresponds to the binding site density (B_T) (average ± standard error, $n > 4$). Note that low signal-to-noise ratios prevented the demonstration of the binding site density in the adventitia. Solid lines are generated from the curve fit binding constants (B_T and K') shown in Table 2 and Eq. 14.

TABLE 2 Binding and distribution constants determined with a nonlinear least-squares Levenberg-Marquardt algorithm

	ϵ'	B_T	K'
Arterial media with intact endothelium	0.61 ± 0.03	4.2 ± 1.7 (μM)	6.8 ± 2.5 (μM)
Arterial media with denuded endothelium	0.70 ± 0.03	2.5 ± 1.1 (μM)	5.0 ± 2.1 (μM)
Adventitia	0.87 ± 0.02	2.2 ± 1.3 (nM)	8.1 ± 5.7 (nM)

Values ± standard error.

through to B_T and K'. The second curve-fitting technique requires the use of more sophisticated computational algorithms to arrive at estimations of the binding and distribution constants. A commercially available software package is used that computes the standard error for each measured constant. The former method, however, provides the required initial estimates used in the latter method.

Although the tissue concentration data are repeatable (Fig. 3), some of the standard errors are relatively high (Table 2). This results in part from the dependence of these particular constants on the subtle convexity of the equilibrium distribution curve, so that small concentration measurement errors create uncertainty. Furthermore, if the scatter in the data is greater than the binding site density, as was encountered with the adventitia, after the subtraction of the soluble component the bound concentration data spread about zero (Fig. 4 *c*). Thus, a low signal-to-noise ratio limits the accuracy of the technique to drug-tissue interactions with a relatively large number of binding sites.

The derivation of the equilibrium distribution method assumed that there was a one-to-one stochiometric relationship between occupied binding sites and bound drug. Although this may be valid for many drugs, for some compounds a single ligand may be able to simultaneously bind several sites, thus limiting the applicability of the law of mass action. This phenomenon may occur in some of the heparin binding sites in arterial tissues. In addition, the partition coefficient (κ) remains unquantified, as it is difficult to measure in complicated structures such as arterial tissues; however, it is expected to be about 1. Despite these possible sources of artifact, these binding constants empirically reflect the drug-tissue interaction and allow for the realistic distinction between bound and soluble drug.

SUMMARY

The equilibrium distribution measurements and subsequent numerical analysis are a useful method of describing the binding of compounds to tissues, not just individual binding sites, and should be applicable to many drug-tissue interactions. Each set of measurements determines the fractional volume of tissue available for drug distribution, binding site density, and affinity of the average binding site. In addition, these constants allow the determination of the bound and soluble fractions of drug from tissue concentration measurements. This information is important as it not only allows for the description of the effects of binding on deposition, but is a prime determinant of the kinetic concentrations produced by novel drug delivery systems.

We thank Professor Douglas Lauffenburger for his careful review of this manuscript, Professor Matthew Nugent for his analytical insight, James Squire for computational assistance, and Renata Yang for help in the laboratory.

This study is supported in part by grants from the National Institutes of Health (GM/HL 49039), the Burroughs-Wellcome Fund in Experimental Therapeutics, and the Whitaker Foundation in Biomedical Engineering.

REFERENCES

Barzu, T., P. Molho, G. Tobelem, M. Petitou, and J. Caen. 1985. Binding and endocytosis of heparin by endothelial cells in culture. *Biochim. Biophys. Acta.* 845:196–203.

Barzu, T., J. L. M. L. V. Rijn, M. Petitou, P. Molho, and G. Tobelem. 1986. Endothelial binding sites for heparin: specificity and role in heparin neutralization. *Biochem. J.* 238:847–854.

Castellot, J. J. J., M. L. Addonizio, R. D. Rosenberg, and M. J. Karnovsky. 1981. Cultured endothelial cells produce a heparin-like inhibition of smooth muscle growth. *J. Cell. Biol.* 90:372–379.

Castellot, J. J. J., D. L. Cochran, and M. J. Karnovsky. 1985a. Effect of heparin on vascular smooth muscle cells. I. Cell metabolism. *J. Cell. Physiol.* 124:21–28.

Castellot, J. J. J., K. Wong, B. Herman, R. L. Hoover, D. F. Albertini, T. C. Wright, B. L. Caleb, and M. J. Karnovsky. 1985b. Binding and internalization of heparin by vascular smooth muscle cells. *J. Cell. Physiol.* 124:13–20.

Castellot, J. J. J., T. C. Wright, and M. J. Karnovsky. 1987. Regulation of vascular smooth muscle cell growth by heparin and heparan sulphate. *Semin. Thromb. Hemost.* 13:489–503.

Clowes, A. W., M. A. Reidy, and M. M. Clowes. 1983. Kinetics of cellular proliferation after arterial injury. I. Smooth muscle cell proliferation following endothelial injury. *Lab. Invest.* 49:327–333.

Edelman, E. R., D. A. Adams, and M. J. Karnovsky. 1990. Effect of controlled adventitial heparin delivery on smooth muscle cell proliferation following endothelial injury. *Proc. Natl. Acad. Sci. USA.* 87: 3773–3777.

Edelman, E. R., and J. M. Karnovsky. 1994. Contrasting effects of the intermittent and continuous administration of heparin in experimental restenosis. *Circulation.* 89:770–776.

Edelman, E., M. Nugent, and M. Karnovsky. 1993. Perivascular and intravenous bFGF administration: vascular and solid organ deposition. *Proc. Natl. Acad. Sci. USA.* 30:1513–1517.

Ellis, S. G., G. S. Roubin, S. B. King, J. S. Douglas, W. S. Weintraub, R. G. Thomas, and W. R. Cox. 1988. Angiographic and clinical predictors of acute closure after native vessel coronary angioplasty. *Circulation.* 77:372–379.

Ellis, S. G., G. S. Roubin, J. Wilentz, J. Douglas, and S. King. 1989. Effect of 18 to 24-hour heparin administration for prevention of restenosis after uncomplicated coronary angioplasty. *Am. Heart J.* 117:777–782.

Glimelius, B., C. Busch, and M. Hook. 1978. Binding of heparin on the surface of cultured human endothelial cells. *Thromb. Res.* 12:773–782.

Haas, K., S. Phillips, A. Comerota, and J. White. 1991. The architecture of adventitial elastin in the canine infrarenal aorta. *Anat. Rec.* 230:86–96.

Hiebert, L. M., and N. M. McDuffie. 1989. The intracellular uptake and protracted release of exogenous heparins by cultured endothelial cells. *Artery.* 16:208–222.

Ip, J. H., V. Fuster, L. Badimon, J. Badimon, M. B. Taubman, and J. H. Chesebro. 1990. Syndromes of accelerated atherosclerosis: role of vascular injury and smooth muscle proliferation. *J. Am. Coll. Cardiol.* 15:1667–1687.

Lehmann, K. G., R. J. Doria, J. M. Feuer, P. X. Hall, and D. T. Hoang. 1991. Paradoxical increase in restenosis rate with chronic heparin use: final results of a randomized trial. *J. Am. Coll. Cardiol.* 17:181A. (Abstr.)

Lovich, M., and E. Edelman. 1995. Mechanisms of transmural heparin transport in the rat abdominal aorta after local vascular delivery. *Circ. Res.* 77:1143–1150.

Murata, K., T. Motayama, and C. Kotake. 1986. Collagen types in various layers of the human aorta and their changes with the atherosclerotic process. *Atherosclerosis.* 60:251–262.

Nugent, M. A., and E. R. Edelman. 1992. Kinetics of basic fibroblast growth factor binding to its receptor and heparan sulfate proteoglycan: a mechanism for cooperativity. *Biochemistry.* 31:8876–8883.

Press, W., B. Flannery, S. Teukolsky, and W. Vetterling. 1986. Modeling of data: nonlinear models. *In* Numerical Recipes. Cambridge University Press, Cambridge. 521–528.

Psuja, P. 1987. Affinity of radiolabeled (^{125}I) heparin and low molecular weight heparin fraction CY 222 to endothelium in culture. *Folia Haematol.* 114:429–436.

Rogers, C., M. J. Karnovsky, and E. R. Edelman. 1993. Inhibition of experimental neointimal hyperplasia and thrombosis depends on the type of vascular injury and the site of drug administration. *Circulation.* 88:1215–1221.

San Antonio, J. D., J. Slover, J. Lawler, M. J. Karnovsky, and A. D. Lander. 1993. Specificity in the interactions of extracellular matrix proteins with subpopulations of the glycosaminoglycan heparin. *Biochemistry.* 32:4746–4755.

Vannucchi, S., F. Pasquali, V. Chiarugi, and M. Ruggiero. 1986. Internalization and metabolism of endogenous heparin by cultured endothelial cells. *Biochem. Biophys. Res. Commun.* 1140:294–301.